LA-UR- 10-01429

Approved for public release; distribution is unlimited.

Title:	Applications and Principles of Photon Doppler Velocimetry for Explosives Testing
Author(s):	Matthew E. Briggs, Larry Hill, Larry Hull, Michael Shinas
Intended for:	14th International Detonation Symposium, April 2010

Los Alamos
NATIONAL LABORATORY
EST. 1943

Form 836 (7/06)

Applications and Principles of Photon-Doppler Velocimetry for Explosive Testing

Matthew E. Briggs, Larry G. Hill, Lawrence M. Hull, Michael A. Shinas

Los Alamos National Laboratory
Los Alamos, New Mexico, United States of America

Abstract. The velocimetry technique PDV is easier to field than its predecessors VISAR and Fabry-Perot, works on a broader variety of experiments, and is more accurate and simple to analyze. Experiments and analysis have now demonstrated the accuracy, precision and interpretation of what PDV does and does not measure, and the successful application of PDV to basic and applied detonation problems. We present a selection of results intended to help workers assess the capabilities of PDV. First we present general considerations about the technique: various PDV configurations, single-signal, multi-signal (e.g., triature) and frequency-shifted PDV; what types of motion are sensed and missed by PDV; analysis schemes for velocity and position extraction; accuracy and precision of the results; and, experimental considerations for probe selection and positioning. We then present the status of various applications: detonation speeds and wall motion in cylinder tests, breakout velocity distributions from bare HE, ejecta, measurements from fibers embedded in HE, projectile velocity, resolving 2 and 3-D velocity vectors. This paper is an overview of work done by many groups around the world.

Introduction – What PDV Is

Photon-Doppler Velocimetry (Heterodyne Velocimetry as it is named overseas) has demonstrated the ability to return high-fidelity signals under difficult fielding situations. The analysis of the results can be done simply and reliably. These qualities earned PDV the nickname "velocimetry for the masses" [1] shortly after its invention, a description borne out by the successes of many non-specialists using PDV since then. This ease of use is allowing workers to replace or supplement lower fidelity diagnostics with PDV. New results are therefore arising from standard tests, such as the cylinder and projectile tests described below. This paper is intended to present the information needed for non-specialists in velocimetry to assess what PDV could do for them, and provide the references they will need to get started.

PDV is a displacement interferometer built from high-bandwidth telecommunications optical-fiber components.[2] One leg of the interferometer is laser light scattered from the surface under test. The simplest implementations of PDV combine this with a reference leg created either from a reflection from one of the optical fiber interfaces along the path to the probe, or from a small portion of the laser light extracted from the fiber before the probe using a fiber splitter,[3] Fig. 1. Displacement along the beam of ½ the 1.5 μm laser wavelength causes a shift of one fringe in the interferometer. The resulting variations in light intensity are detected with a photodiode and recorded on a high-bandwidth oscilloscope channel.

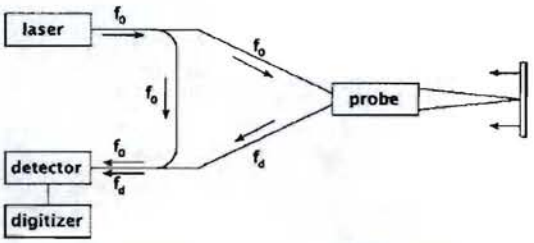

Fig. 1. The basic PDV design is a fiber Mach-Zender interferometer. Light at frequency f_0 interferes with light at frequency f_d at the detector and is recorded by a digitizer. f_d is Doppler-shifted away from f_0 by the motion of the surface at right, so that one fringe corresponds to motion of the surface toward the probe of $\lambda/2$. The probe can be simply the end of a fiber or a fiber with lenses attached, and serves both to deliver the light to the target and to collect the backscattered light.

In the above design, fringes appear when the object begins to move, and the frequency of the fringes is the rate at which the surface moves through a distance of $\lambda/2$ along the probe beam. Ref. 2—5 describe the creation of the signal in detail as a beat frequency between f_0 and f_d. A 1 GHz signal corresponds to a velocity of $\lambda/2 \cdot 10^9 =$ 0.75 km/s. The typical PDV system has 15 GHz analog bandwidth detectors and 8 GHz analog bandwidth digitizers. Bandwidths up to 20 GHz are available, corresponding to a speed of 15 km/s.

The direction of motion cannot be determined because the analysis does not distinguish between increasing and decreasing phase. However, if the reference beam is shifted away from frequency f_0 with an acousto-optic frequency shifter or a 2nd laser,[4] zero motion now appears at the modulation frequency. This can move the signal into a more optimum frequency range for the phenomena under investigation, and allows the direction to be determined by whether the signal appears above or below the modulation frequency. Dynamic range is reduced (see Up or Downshifting, below).

Example Signal and Analysis

One can attempt to extract the position as a function of time directly from the single channel of data obtained from the design above, but amplitude variations and changes in baseline render such an extraction difficult in almost all cases. Fig. 2 shows the digitizer record for a probe looking normally at a metal plate on a slab of high explosive that is detonating sideways along the slab. Note how the fringes oscillate about a center that shifts up and down at all time scales, and the amplitude varies similarly quickly. The shifts up and down are presumed to be variations in the intensity as the surface quality changes and tilts, and the amplitude variations are presumed to be speckle. Only when these variations are tiny, as in 1-D motion of polished surfaces, have algorithms to extract position ("unwrap" the phase) from a single-channel measurement like this succeeded. Extracting position directly from the fringes has been done successfully by recording multiple phases of the signal, see Quadrature Techniques below.

Note the physics that one can pick out of the raw signal by inspection: The motion begins a slow acceleration, as shown by the slow fringes in the upper left inset, which is a zoom of the start of motion. The shock arrives ~200 ns later, emerging in about 10ns from the slower variations, as shown in the upper right.

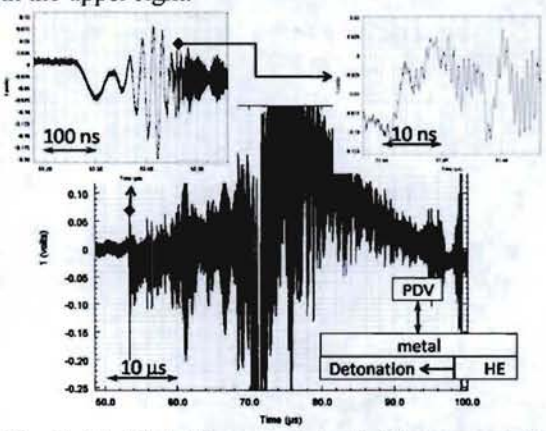

Fig. 2. Big Plot: The complete digitizer record for a flat plate driven by a detonation travelling parallel to the plate. The start of motion is expanded on the upper left, showing a slow initial acceleration before the arrival of the shock, and the shock arrival is shown in the upper right. Note the amplitude variations (speckle) and baseline shifts (reflectivity and tilt.)

The standard approach to extracting velocity v very easily and accurately from PDV data is to apply a sliding Fast-Fourier Transform and convert the frequency spectrum to motion using $v = 2f\lambda$, where f is the frequency of the fringes, i.e., the beat frequency between the reference and test legs, and λ is the wavelength of the laser. The measured quantities that determine the accuracy of this formula are the wavelength of the laser, the time base of the oscilloscope, and the linearity of the detection. These three quantities have proven to be so ideal in practice that they do not limit the accuracy of the above analysis. The limitations turn out to be noise fraction and the width of the Fourier Transform Window relative to the fringe period, as discussed below. As a result, velocity measurements with PDV are inherently simple and accurate, demonstrated to date to about 0.1%.[5] The result of such an analysis is shown in Fig 3.

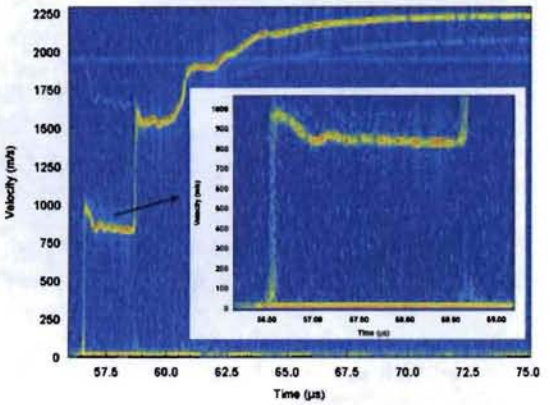

Fig. 3. The spectrogram for the signal in Fig 2 shows coasting after the initial shock, which suggests spall, along with a hint of ringing from which one can obtain the spall thickness, re-shock and then gradual acceleration to the terminal velocity corresponding to all the explosive energy having been delivered to the metal. The initial slow acceleration evident in Fig. 2 is intrinsically difficult for FFT analysis, and is barely visible in this figure.

Fast Fourier Transform Analysis

Sliding FFT analysis of data such as that shown above has been shown to give accurate and precise velocities, despite the non-ideal behavior of the raw signal. Jensen et al. used 1-D gun shots to demonstrate accuracy and precision to < 0.1% in a steady velocity.[5] Accuracy during slewing is more difficult to prove, but in the same paper these authors showed agreement between the independent diagnostic VISAR at this same level.

The basic principle of the sliding FFT is to apply an FFT analysis to a small time segment of the data of duration τ, assign the resulting frequency spectrum to the center of that time segment, and repeat this for time segments covering the whole record. To minimize artifacts, the data are always turned on and off smoothly within τ by multiplying by a window function. The ideal choice of window function depends on the noise, but not dramatically.[6] Taking the Hamming window as a good general purpose choice, note that only the center ~20% of the window contributes significantly to the result. A common analysis approach is then to apply the Hamming window of width τ, but move only $\tau/8$ between FFT points. The vertical bands in Fig. 5 are spaced by this amount (τ is actually 8x the width of one of these bands), and the start of motion can be seen to contaminate primarily just one time step early. See the appendix in Ref. 5 for an excellent introduction to PDV analysis.

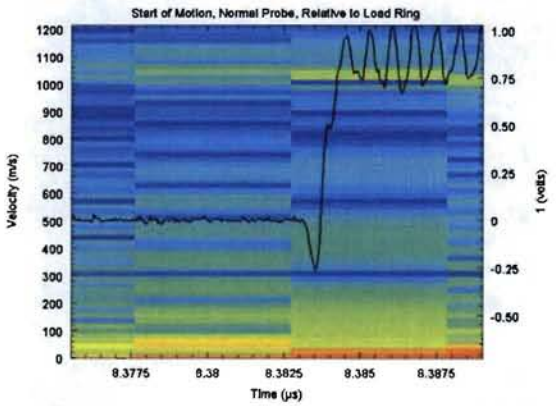

Fig. 4. The raw signal (right y-axis) overlying the spectrogram (left y-axis) at shock arrival for normal incidence shows the resolution in start of motion obtainable from the raw signal, and the smearing effect of the bin size in the FFT.

Accuracy and Precision of FFT Analysis

Extracting frequencies from a time record forces us to compromise between frequency

(velocity) resolution and time resolution. The time resolution is set by τ, but the frequency resolution is set by $1/\tau$; the number of cycles that are averaged by the FFT is limited to at most $f\tau$. One expression of this is the uncertainty relation between the width of the Gaussian frequency peaks δf resulting from the FFT analysis and the analysis window width τ, $\delta f \cdot \tau \geq 1/4\pi$. Fig. 4 shows the smearing of a frequency change in time. From the raw signal, we can resolve the start of motion to $\pm$ 0.1 ns (!), but the time bins of the FFT smear the start of motion over about 10 ns. Noise plays a key role in this trade-off, because the FFT requires more oscillations of a noisy signal to determine a frequency.

The frequency resolution will be best when the frequency is present throughout the FFT window width τ; changes faster than τ result in fewer cycles at a given frequency for the FFT to average. Guidelines for the precision to expect in this best case in the presence of noise in the time record at a fraction σ have been put forward by Dolan, using Monte-Carlo calculations on synthetic data.[6] He finds that the uncertainty relation is too conservative, because a Gaussian fit locates the peak frequency more accurately than the width given by the uncertainty relation. His numerical study finds that: 1.) A systematic bias toward zero frequency arises for frequencies $f < 1/\tau$, i.e., the FFT needs at least one full cycle; 2.) For $f > 1/\tau$, accuracy effects are less than noise effects, i.e., the accuracy is better than the precision, and the precision is roughly independent of frequency, with a lower limit of

$$\delta f = \sqrt{\frac{6}{N}} \frac{1}{\pi\tau} \sigma . \quad (1)$$

σ as before is the noise fraction in the time record, τ is the width of the FFT window, and N is the number of samples in this window. The actual precision will not be quite this good and depends on the windowing used. The lack of frequency dependence in (1) suggests that the increase in the number of cycles available to the FFT at higher f during τ is offset by the reduced number of samples in the time record per cycle.

The forgoing discussion suggests that up-shifting the frequency will improve the time resolution and lower the minimum Doppler shift measureable without bias simply by mapping it to a higher frequency; Dolan demonstrates the improved time resolution for a velocity step of 266 m/s.

Forward Modeling

Certain measurements, such as measuring the velocity pull-back after shock in order to determine material strength, require extracting as much time resolution as possible from the data. If the function v(t) is known, then the parameters of the function can be fit to the observed spectrogram. Furlanetto[7] has demonstrated using synthetic data that such an approach improves the precision by an order of magnitude without introducing systematic errors, *provided* the correct function is chosen. He observed that choosing an incorrect function can lead to systematic errors that are not evident in result, and so such an analysis must be approached with great caution, but does extract greater precision and accuracy if done correctly.

Multiple Velocities

A strength of FFT analysis lies in revealing the presence of multiple frequencies. The results of FFT analysis of PDV data have revealed velocity spectra above shocked surfaces and bare HE, simultaneously seeing the surface below, as well as doubly and triply Doppler shifted light from multiple Fresnel reflections in window experiments. Usually, understanding which curve represents what behavior in the experiment is obvious. However, the set of frequencies to expect from multiple reflections can be quite subtle. This has been worked out in Ref. 4, in order to understand symmetric impact experiments. An excellent exercise in understanding the analysis of PDV signals and appreciating the power of PDV is to understand the various velocities that appear and disappear during the course of the symmetric impact experiment shown in Fig 5 of that reference.

Analysis Software

Many workers quickly make their own analysis software using canned FFT/power spectra routines available in MatLab, Igor, etc. For a publicly available set of MatLab-based routines, contact Ref. 8.

What Types of Motion are Detectable with PDV?

Material can approach the probe either by having a component of velocity along the probe beam, or by entering the beam transversely as would happen during the transverse motion of an angled surface, Fig 5.

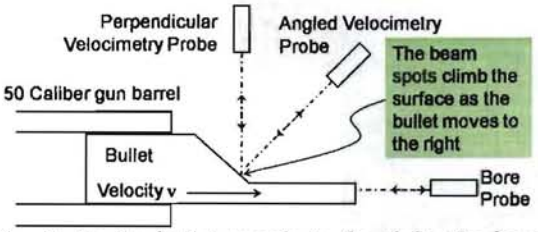

Fig. 5. As the bullet travels to the right, the bore probe is approached by its beam spot, while the angled and perpendicular probes see a constant location on the flat region, then are approached as the spots climb the slope.

For VISAR and Fabry-Perot, we know that only when the individual scatterers have a component of velocity along the beam will there be a non-zero velocity.[9] Since one thinks of these techniques as based on the Doppler frequency shift, the result is expected; the perpendicular probe reports zero velocity despite being approached by the beam spot because the scatterers are entering the beam transversely, i.e., with no Doppler shift in the direction of observation.

However, PDV is a displacement interferometer, so one might expect the approach of the beam spot towards the perpendicular probe to be seen as a non-zero velocity. We performed this test, and found instead zero velocity in the perpendicular probe, and the angled probe measured the component of the bullet velocity along its beam for both the flat part of the bullet where the beam spot is not moving, and the angled part of the surface where the spot approaches the beam.[10]

Similarly, if one investigates the motion of a rotating circle or cam, Fig. 6, on finds a constant velocity equal to the component of the velocity vector of the individual scatterers along the beam, regardless of the motion of the beam spot.[11]

These results mean that *PDV signals can be attributed unambiguously to actual particle motion along the beam*, as opposed to being an unknown combination of that and material entering the beam transversely nearer or farther from the probe. This is an important simplification to the interpretation of PDV data, but is a puzzle, since PDV is a displacement interferometer.

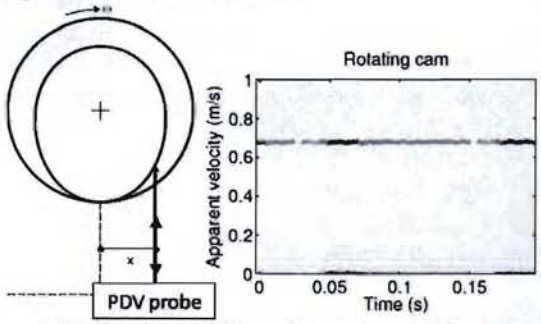

Fig. 6. The PDV probe measures the same non-zero velocity at a given distance x from the center of rotation, regardless of whether it is striking the egg-shaped or circular surface. The illuminated spot is stationary when the disk is the target, and oscillates towards and way from the probe when the egg-shape is illuminated

.

The reason PDV does not sense the approach of the beam spot if it arises from transverse motion is explained by Fig. 7. All non-polished surfaces that would return a signal at an angle will have surface roughness much greater than the wavelength of the PDV light, 1.5 μm, and so the phase will not progress but vary randomly. Discussion of this as a sum of phasors is in Ref. 10, as a transit time formulation Ref. 11, and a start at an (x,t) formulation in Ref. 12

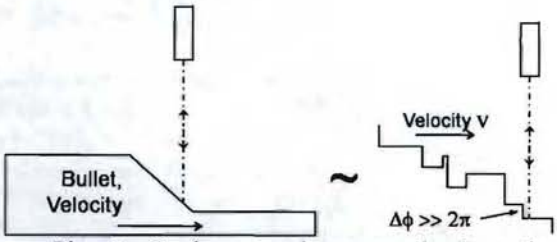

Fig. 7. Surface roughness randomizes the phase progression as the spot moves up the surface, so that PDV, despite being a displacement interferometer, sees nothing when material approaches the probe transversely.

Position from Integrated Velocity

Finding the position of material as a function of time is important in the modeling of explosive systems whose performance depends on material arrival times. Provided material does not approach the probe due to transverse motion as just discussed, or such motion is known from other diagnostics or modeling, the integrated PDV velocimetry signal provides good position data. (See also "Quadrature Techniques", below.)

The accuracy of position found from integrating the velocity is a 1-D random walk problem. The integral is calculated as a sum of $v(t)\Delta t$, with Δt the time shift in the sliding FFT, i.e., the time between frequency samples. At each of these time steps a random displacement error of most probable amplitude $\sigma_v \Delta t$, the standard deviation of the velocity, is added or subtracted. The most probable magnitude of error therefore grows like the 1-D random walk with step size $\sigma_v \Delta t$, i.e, $\sigma_x = \sqrt{N}\sigma_v \Delta t$, where N is the number of velocity samples being integrated.[13] As a fraction of the total displacement, this error decreases like $1/\sqrt{N}$. However, as an absolute error in position, the error grows like $\sqrt{N}$. This has been worked out and modeled for a variety of noise levels in Ref. 14. The cylinder tests discussed below demonstrate an error of < 0.1 mm on a 30 mm run.

PDV Designs for Improved Performance

More Signals/Channel by Using Optical Delay

Although 1 km of fiber gives only about 5 μs delay, the ~monotonically increasing behavior of most velocimetry records allows such a slight delay to be quite useful.[15] Provided one does not saturate the detector with too much light (not usually a problem), the delayed signal is always a bit below the first, and the two signals are easily extracted from the same spectrogram. Note that if one uses the probe back-scattering as the reference beam, the requirements on the coherence length are less stringent then in a design with a separate reference beam, although usually the coherence length is plenty long enough and the demonstration was done in the configuration with a separate reference beam.

Up or Downshifting of the Reference Beam

One of the most powerful improvements to the basic PDV design is to be able to shift the frequency of the reference beam f_0 up or down, to $f_0 \pm f_m$.[4,16,17] Light returning from the probe will have frequency $f_0 + f_d$, so that the interference signal will be at frequency $\pm f_m - f_d$. This means that zero motion now appears at frequency f_m, and if one picks an up-shift, i.e., a positive f_m, motion toward the probe shows up below f_m, and away from the probe above f_m. The important advantages of this are that the direction of motion is known, and that slow motions can be resolved with good time resolution by a standard FFT because they are represented by a higher frequency. The penalty is in bandwidth; for the signs chosen above, motion away has lost 1 GHz out of the full bandwidth of the system, and motion towards is limited to a bandwidth of 1 GHz before reflecting off of zero. Fig. 8 shows an experiment with motion towards and away from the probe, as measured by both the standard method and the up-shifted method.

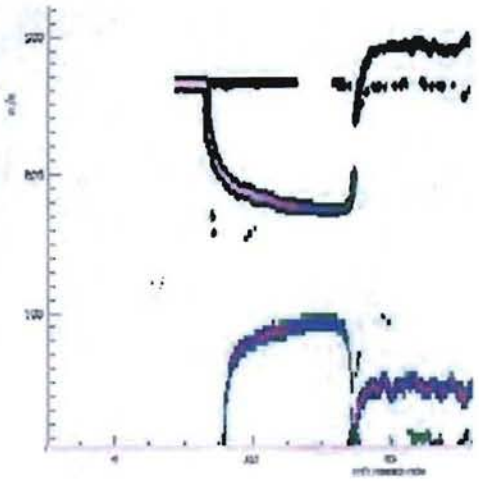

Fig. 8. Up-shifting allows a single PDV channel to reveal that the lower signal, recorded without up-shifting, is actually motion towards and away from the probe (upper signal.)

Two strategies have been shown to work for this. For frequency shifts in excess of 1 GHz, a second laser is used in place of f_0 and tuned to the frequency difference desired. That approach requires the frequencies of both lasers to be stable to a fraction of the difference frequency over the ~100 μs of a typical experiment in order to know the frequency that corresponds to zero velocity. Not all the lasers commonly in use for PDV have such stability. Alternatively, an acousto-optic frequency shifter inserted in the reference leg can create up to 1 GHz shift in f_0. This approach relaxes the requirements on laser stability, depending only on the stability of the rf drive of the acousto-optic modulator, which is sub 0.1%.

Quadrature Techniques

By dividing a signal into two or three copies, each phase shifted with respect to one another, the problem of extracting the phase of the PDV signal (i.e., position) in the presence of amplitude variation and baseline shifts has been overcome.[18,19] The potential advantages to this are improved time resolution, resolving the direction of motion, and improved position measurements. The cost and complexity increase significantly, since the oscilloscope channels are the most expensive part of a PDV system, and the quadrature data analysis is more complicated. However, Dolan and Jones have worked out the analysis and demonstrated successful application, and have developed a software package to do the analysis.[20]

Measuring the Velocity Vector

A single velocimetry probe resolves only the component of velocity along its beam direction. (If it detects coherent light from a different probe, it measures the average of the component of velocity along the other probe and the component of velocity along its own beam.) To find the direction of motion using PDV, one must therefore use multiple probes measuring the velocity at the same point in space from different angles. The metrology of this type of measurement can be done accurately and easily using a beam position sensor and translation stage to align beams from different probes at a specific location and measure the angles of the beam. Fig. 9 shows a demonstration of this technique in which the sample was driven by a detonation travelling straight up and centered on probe 1. Light from probe 1 shows up as signal in the tilted probes at a slightly higher velocity than their own signals because it has only one cos(30°) projection instead of two (they were all illuminated by the same laser and so were coherent). This mark confirmed the alignment and the time at which to compare velocities. The velocities measured by the tilted probes agreed to within ± 1° of the predicted 30°, with the error set by the weak signals of the tilted probes from what was a somewhat specular surface. Note that the use of the beam position sensor allowed us to align the 0.1 mm beam diameters on each other within ±0.025mm at a height of 1mm above the sample.

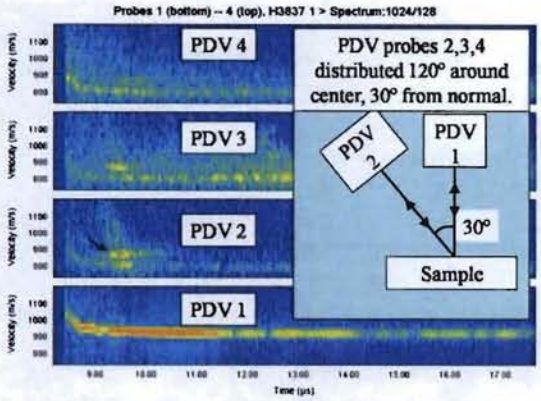

Fig. 9. By aligning multiple probes to interrogate a single point in space, the velocity vector can be resolved in three dimensions. Probes 2—4 suffice to define the angle and agreed within measurement error of 1°, probe 1 provided a check and a convenient marker verifying overlap on probes 2—4, shown by the arrow on PDV2.

Probe Selection

There are basically three types of probes from which to choose. When the motion of interest spans only a few mm, and the spot size is does not need to be small, the bare end of a fiber polished to 8°, such as the end of an FC/APC connector works fine. When one wants to track motion all the way to probe impact with good signal, and a spot diameter of just under 0.5 mm is small enough, collimated probes are the solution. These are also advantageous because of lower cost ($30--$50) and small size (down to 1mm diameter.) For experiments in which shock travels laterally down the target, the start of motion is smeared by the time to travel across the beam spot. In addition, the resolution on the start of motion is strongly influenced by signal strength. Both of these problems are minimized by using a focusing probe, which can produce spot sizes down to .050 mm routinely and has very strong signal return in a narrow range around its design working distance. These probes however are larger, ~8mm in diameter, and run $150.

We have measured light collection efficiency in a standard setup for about a dozen different probes.[21] Representative curves for a focused probe and collimated probe are shown in Fig. 10. The focused probe is 10dB more efficient at its peak, and is better over ± 10mm from the peak. The final signal strength in a given test depends on a great many factors that we do not quantify; how specular is the back reflection, how much will the change in the tilt of the surface effect the return, and what happens to surface quality as the experiment progresses. By having these efficiency curves, we can build on our experience to try to reduce some of this uncertainty when designing new tests. Several manufacturers are in common use, AC Photonics, Lightpath, Oz Optics, and Thorlabs to name a few.

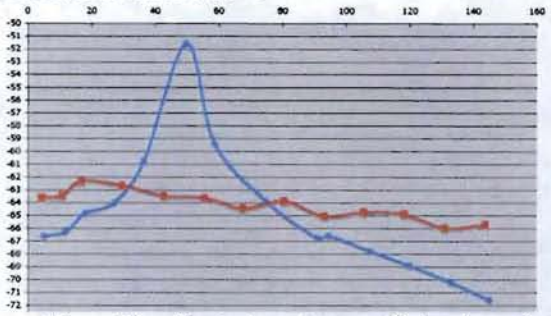

Fig. 10. Typical return efficiencies for Focused (blue) and collimated (red) commercial probes. The scales are 0—160 mm horizontal, and -50 to -75 dB power returned vertical.

Probe Alignment

Probe alignment is a compromise between surface tilt and direction of travel. Signals are strongest when the probe is aligned normal to the surface, and the velocity measured requires no cos(θ) correction when the beam is aligned along the direction of travel. However, unless the detonation is normal to the surface, the surface will travel in a different direction than it tilts. A simple model turns out to work well at predicting the tilt and velocity directions,[22] with the result that in the steady state the velocity angle relative to the original normal is ½ the tilt angle, with a typical value of about 6°. The decision of how to align then depends primarily on the most important aspect of the data record. If resolving start of motion is most important, then one accepts the loss of light from the 12° tilt and the cos(6°) = .995 correction, and simply aligns normal to the surface. If signal strength after the start of motion

is most important, for example to integrate to get the total distance or to resolve ringing or other fine structure during the flight, then one would align at 12°, again making a cos(6°) correction. Often people compromise and align right along the velocity at 6°.

Applications

Cylinder Tests

One of the standard tests for HE performance is a cylinder test.[23] A metal cylinder, typically 1 inch diameter, 0.1 inch wall thickness Cu, is filled with the HE to be tested and detonated from one end. The detonation speed and wall expansion speed are measured, and can be used with simple equations to determine the specific energy of the explosive. Traditionally the detonation speed has been measured with shorting pins running up the side of the cylinder, and the wall expansion speed has been measured with a streak camera at a standard location about 2/3 along the detonation.

PDV could improve both measurements. The start of motion is ± 0.1 ns for strong signals, as compared to about 10 ns for pins. Both the time resolution and accuracy of the velocity measurement greatly exceed that of a streak camera over the long time scale of a cylinder test.

We performed a series of cylinder tests on liquid explosives, done with both the traditional pins and an array of PDV probes along the length of the cylinder. The setup is about the same for the two techniques, with a telescope mounted on a precision vertical translator for accurate beam spot and pin wire height measurements.

The detonation speeds measured by fitting the height vs. the start of motion time agreed to .05%, suggesting that both techniques are accurate to this level if done with appropriate care. The poorer time resolution of the pins was compensated by their larger number compared to the number of PDV probes, so the precision of the fit was comparable. The choice of PDV vs. pins for detonation speed measurements will therefore depend on the value of having spectra along the cylinder, e.g., for detailed modeling vs. which is easiest for the experimenter.

The wall velocity measurements from the PDV were an order of magnitude more precise than the streak camera, and matched the streak camera record within measurement error. The analysis of the PDV data was more straightforward and revealed much more dynamic information. PDV appears to be the clear choice for the wall velocity measurement in these kind of tests.

In the tests reported in Ref. 23, we had careful metrology on the travel distance to the probe, and found that the integrated velocity agreed with the known travel distance to ~0.5%, about the measurement error. The comparison between the streak camera and PDV data for these shots is in progress.

PDV will clearly improve the precision of cylinder tests. Whether it will improve the accuracy depends on further work to understand the systematic errors in the equations used to extract the specific energy from the measurements.

Embedded Fibers

Embedding fiber inside materials has allowed velocimetry measurements inside of detonating and shocked systems.[4,24,25] A talk detailing this work is being presented by Hare, Holtkamp and Strand at this symposium. Here we note that the onset of detonation in liquid explosives, and the behavior of shocks and detonations crossing material interfaces and gaps have been revealed using this strategy.

Ejecta and Bare High Explosives

PDV's ability to measure velocity distributions has inspired several workers to investigate bare high explosives and ejecta produced by shocked surfaces. Looking directly at an explosive, and at thin foils of aluminum or Teflon stuck to the HE surface with a gooey medium, reveals velocity spectra from both under-driven (i.e., burning) and over-driven (i.e., detonating) tests.[26] In the under-driven case, a broad spectrum observed by looking directly at the HE is confined to a narrow spectrum tracking the lower velocities by the aluminum foil, and to a narrow spectrum tracking the high velocities by the Teflon tape, Fig. 10. A detail of this study is that we found better success using focused probes rather than collimated probes.

Results from the over-driven case were much

weaker, in part because the speeds were outside the bandwidth of the PDV system. We did however detect a weak signature looking at Teflon tape, with the same shape as the right-hand spectrum in Fig 10, but at about 9 km/s.

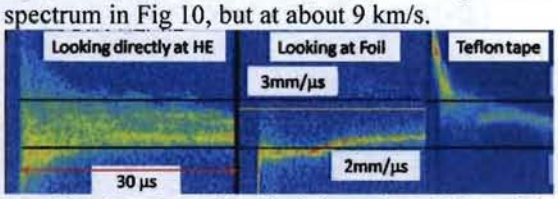

Fig. 10. Three identical shots, bare HE on left, aluminum foil on the HE in the middle, Teflon tape on the HE at right. The HE was burning, not detonating (under-driven.) The spectrograms suggest that the foil tape rides the bottom of the velocity spectrum, while the Teflon is riding on the higher speeds in the spectrum.

The shape of the upper end of the velocity spectrum on the left and right hand plots in Fig. 10 suggests air drag slowing the particles. This phenomenon is treated quantitatively in Ref. 4, where the shape of the deceleration is shown to select a size range for particles ejected from a shocked tin surface. These authors ask the question of whether one could model the ejecta well enough to map the intensity of the velocity spectra to the number of particles traveling at a given velocity. We do not know of any progress on this question, but the complexities of this problem have been highlighted in the literature.[27]

Finally, we succeeded in recording the onset of detonation in bare HE from projectile impact, Fig. 11.

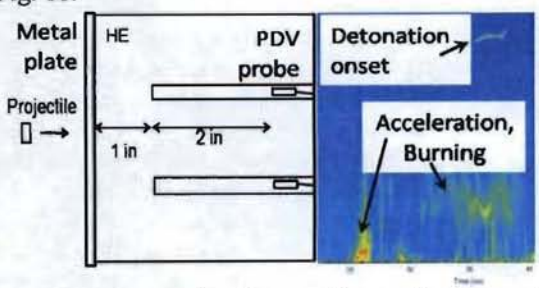

Fig. 11. A projectile travelling ~ 1km/s struck the HE and gave rise to signals in the PDV that suggest an initial acceleration and burning at 200 – 500 m/s, and a detonation 10 μs after start of motion, at 7.7 km/s, correct for the HE used. The PDV probes were collimated probes inserted 2 inches from the ends of blind holes in the HE.

Projectiles

We have captured the entire process of rupture disk bursting, acceleration down the barrel, and free flight with a single probe looking down the barrel of a .50 caliber gun. The data in Fig 12 are from the "bore probe" shown in Fig 5. Note that in other experiments we have successfully picked up a bullet in mid-flight by triggering on the signal, and that one can view the bullet from behind if the down-range location is unavailable. PDV has also been used to measure the balloting (sideways oscillations) of projectiles[28]

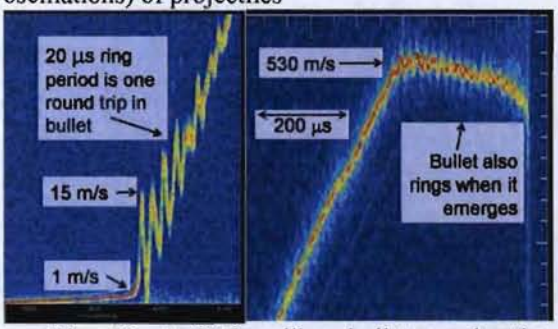

Fig. 12. A 0.50 caliber bullet accelerating (left) and leaving (right) the barrel. A slow ramp leads to the 1 m/s speed noted on the left, which we attribute to the expansion of the rupture disk. The ringing presumably marks the rupture of the disk shocking the bullet. Note that the bullet also rings when it leaves the barrel.

References

1. Hotkamp, D., private communication shortly after his first successful PDV experiments.
2. Strand, O.T., Goosman, D.R., Martinez, C., Whitworth, T.L., and Kuhlow, W.W., "Compact System for High-Speed Velocimetry Using Heterodyne Techniques," Rev. Sci. Inst., Vol. 77, pp.
3. Holtkamp, D.B., "Survey of Optical Velocimetry Experiments – Applications of PDV, a Heterodyne Velocimeter," *Proceedings of the 2006 International Conference on Megagauss Magnetic Field Generation*, Santa Fe, New Mexico, 2006

4. Mercier, P., Benier, J., Frugier, P.A., Contencin, G., Veaux, J., Lauriot-Basseuil, and S. Debruyne, M., "Heterodyne Velocimetry and Detonics Experiments," Proc. of SPIE Vol 7126, 2009.
5. Jensen, B.J., Holtkamp, D.B., Rigg, P.A. and Dolan D.H., "Accuracy Limits and Window Corrections for Photon Doppler Velocimetry," J. Appl. Phys., Vol 101, 2007.
6 . Dolan, D.H., "Accuracy and Precision in Photonic Doppler Velocimetry," in preparation.
7. Furlanetto, M., Los Alamos National Laboratory P-Division Memo P-23:06-32, June 27, 2006, and private communication.
8. Scott Levinson, levinson@iat.utexas.edu.
9. Goosman, D.R., Frank, A.M, Chan, H.H., and Parker, N.L., "Fabry-Perot Velocimetry Techniques: is Doppler Shift Affected By Surface Normal Direction?" Proc. SPIE Vol 427, p. 127-135, 1983.
10. Briggs, M., Hull, L., and Shinas, M., "Fundamental Experiments in Velocimetry," Proceedings of the Conference on Shock Compression of Condensed Matter, AIP Conf. Proceedings 1195, Nashville, TN, 2009
11. Dolan, D.H., "What Does "Velocity" Interferometry Really Measure?" Proceedings of the Conference on Shock Compression of Condensed Matter, AIP Conf. Proceedings 1195, Nashville, TN, 2009

12. Mercier, P., Benier, J., Azzolina, A., Lagrange, J.M., and Partouche, D., "Photonic Doppler Velocimetry in Shock Physics Experiments," J. Phys. IV France, Vol. 134, pp 805-812, 2006.
13. Reif, F., *Fundamentals of Statistical and Thermal Physics,* McGraw-Hill, New York, 1965.
14. Strand, O., "Understanding Distance Uncertainties Using PDV on Dynamic Experiments," PDV Workshop, Austin, TX, 2009*
15. Mercier, P. & colleagues, private comm.
16. Jones, S, Chandler G., Covert, T., Adrian, H., and Sibley, A., "Directional Velocity Measurements Using Frequency-Shifted Reference Leg," PDV Workshop, Austin, TX, 2009*
17. Diaz, A., Gallegos, C., Teel, M., Berninger, M., and Tunnell, T., "Analysis of Optical Upshifted PDV Data," PDV Workshop, Austin, TX, 2009*
18. Dolan, D.H., and Jones, S.C., "Push-Pull Analysis of Photonic Doppler Velocimetry Measurements," Rev, Sci. Instr., Vol 78, 2007.
19. Gallegos, C., Marshall, B., Teel, M., Romero, V., Diaz, A., and Berninger, M., "Comparison of Triature Doppler Velocimetry and VISAR," PDV Workshop, Austin, TX, 2009*
20. D.H. Dolan and S.C. Jones, THRIVE: a data reduction program for three-phase PDV/PDI and VISAR measurements, Tech. Rep. SAND2008-3871, Sandia National Laboratories (2008), available at http://dx.doi.org/10.2172/942210.
21. Shinas, M., Briggs, M., and Hare, S., "Update on PDV Probe Efficiency Study," PDV Workshop, Austin, TX, 2009*
22. Kennedy, J., "The Gurney Model for Explosive Output for Driving Metal, in *Explosive Effects and Applications,* edited by Zukas, J. and Walters, W., pp. 221-255, Springer-Verlag, New York, 1998.
23. Hill, L.G., Mier, R., and Briggs, M.E., "PBX 9404 Detonation Copper Cylinder Tests: A Comparison of New and Aged Material," Proceedings of the Conference on Shock Compression of Condensed Matter, AIP Conf. Proceedings 1195, Nashville, TN, 2009
24. Goosman, D.R., Wade, J.T., Garza, R., Avara, G.R., Crabtree, T.R., Rivera, A.T., Hare, D.E., Tolar, D., Bratton, B.A., "Optical Probes for Continuous Fabry-Perot Velocimetry Inside Materials," Proc. SPIE Vol 5580, 517 (2005).
25. Hare, D.E., Holtkamp, D.B., and Strand, O.T., "Embedded Fiber Optic Probes to Measure Detonation Velocities Using the Photonic Doppler Velocimeter," to be presented here at the 14th International Detonation Symposium, Coeur d'Alene, ID, 2010.
26. Tasker, D.G., Whitley, V.H., and Lee, R.J., "Electromagnetic Field Effects in Explosives," Proceedings of the Conference on Shock Compression of Condensed Matter, AIP Conf. Proceedings 1195, Nashville, TN, 2009
27. Buttler, W.T., Comment on "Accuracy Limits and Window Corrections for Photon Doppler Velocimetry, " J. Appl. Phys. Vol 103, 2008.

28. Levinson, S., Satapathy, S., "Measuring Projectile Balloting in a Gas Gun Launcher," PDV Workshop, Austin, TX, 2009*
* Talks available at http://www.iat.utexas.edu/pdv/agenda.html.